

Rhodium-Catalyzed Formation of Silylcarbamates from the Reaction of Secondary Amines with CO₂ and Hydrosilanes

Jefferson Guzmán, Adrián Torguet, Pilar García-Orduña, Fernando J. Lahoz,
Luis A. Oro and Francisco J. Fernández-Alvarez*

*Departamento de Química Inorgánica-Instituto de Síntesis Química y Catálisis
Homogénea (ISQCH), Universidad de Zaragoza – CSIC, Facultad de Ciencias
50009, Zaragoza – Spain. E-mail: paco@unizar.es.*

Abstract

The reaction of (4-methyl-pyridine-2-iloxy)dimethylsilane ($\text{NSi}^{\text{Me}}\text{-H}$, **1**) with $[\text{RhCl}(\text{coe})_2]_2$ gives the rhodium(III) complex $[\text{Rh}(\text{Cl})(\kappa^2\text{-NSi}^{\text{Me}})]$ (**2**), which reacts with a stoichiometric amount of AgCF_3CO_2 to afford $[\text{Rh}(\kappa^2\text{-CF}_3\text{CO}_2)(\kappa^2\text{-NSi}^{\text{Me}})_2]$ (**3**). Complexes **2** and **3** have been fully characterized by elemental analysis and NMR spectroscopy. The solid-state structure of **3** has been confirmed by X-ray diffraction analysis. Moreover, the activity of complex **3** as catalyst for the reaction of secondary amines with CO_2 (3 bar) and hydrosilanes has been studied. The outcomes of these catalytic studies show that under these conditions complex **3** promotes the selective formation of silylcarbamates.

Keywords

CO_2 -reduction, Rhodium, Homogenous Catalysis, Silylcarbamates, Hydrosilylation

1 Introduction

Pyridine-2-iloxy-silyl based anions could be considered promising ligands due to their electronic and steric versatility, which includes their potential as monoanionic bidentate (κ^2 -NSi), tridentate (κ^3 -N₂Si) or tetradentate (κ^4 -N₃Si) ligands [1,2]. In addition, their steric hinderance, sigma donor ability of the nitrogen atom(s) and *trans* influence of the silyl group could be easily tuned by choosing the proper substituents at the pyridinic ring(s) and/or the silicon atom (Figure 1). However, this type of ligands presents the disadvantage that the functionalized silanes used as precursors are very reactive and hydrolyze easily in the presence of traces of moisture. This may be one of the reasons why the transition metal coordination chemistry of these type of ligands has been scarcely explored so far [1,2].

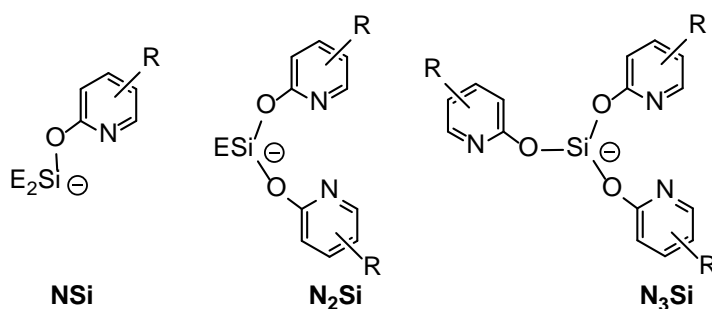


Figure 1. Examples of monoanionic pyridine-2-iloxy-silyl based ligands (E and R alkyl or aryl groups).

In this context, it is worth mentioning that in recent years we have demonstrated that rhodium and iridium complexes with pyridine-2-iloxy-silyl based ligands are excellent catalysts for hydrosilylation and/or silylation processes [2]. For example, iridium-*(fac- κ^3 -N₂Si)* complexes (N₂Si = *fac*-bis(pyridine-2-iloxy)methylsilyl or *fac*-bis(4-methylpyridine-2-iloxy)methylsilyl) are effective catalysts for the solvent-free selective reduction of CO₂ to silyl-formates [3], the hydrolysis of hydrosilanes to

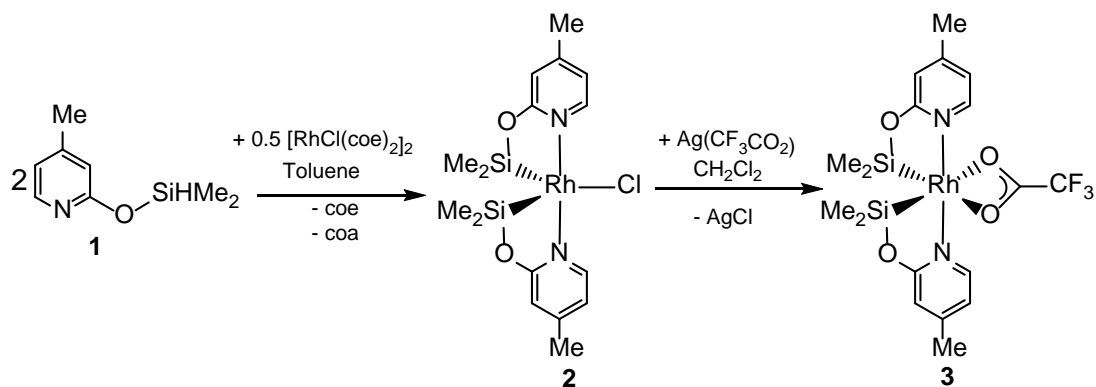
afford the corresponding silanol and hydrogen [4], the synthesis of silylamines by dehydrogenative silylation of secondary amines [5], the synthesis of silylesters by dehydrogenative silylation of carboxylic acids [6], the synthesis of silylphosphanecarboxylates by insertion of CO₂ into the P-Si bond of silylphosphanes [7] and the synthesis of silylcarbamates from insertion of CO₂ into the N-Si bond of silylamines [5]. In addition, rhodium-(*fac*-κ³-N₂Si) (N₂Si = *fac*-bis(pyridine-2-iloxy)methylsilyl) species catalyzes the formation of silylenolethers by dehydrogenative silylation of acetophenone derivatives [8].

Examples of hydrosilylation catalysts based on iridium complexes with monoanionic bidentate NSi ligands have also been reported. Thus, Ir-(κ²-NSi^{tBu}) (NSi^{tBu} = (4-methylpyridine-2-iloxy)diterbutylsilyl) species are effective catalysts for the selective reduction of formamides to *O*-silylated hemiaminals or to amines [9]. Moreover, Ir(κ²-NSi^{Me})₂ (NSi^{Me} = (4-methylpyridine-2-iloxy)dimethylsilyl) complexes are effective catalyst precursors for the selective reduction of CO₂ to silylformate or methoxysilane [10]. Herein, the synthesis and characterization of Rh-(κ²-NSi^{Me})₂ species together with the study of their potential as catalysts for the reaction of secondary amines with CO₂ and HSiMe₂Ph is described. The outcomes of these studies revealed that Rh-(κ²-NSi^{Me})₂ species promoted the selective formation of silylcarbamates from the reaction of aliphatic secondary amines with CO₂ and hydrosilanes.

2. Results and Discussion

Synthesis and characterization of the rhodium catalyst precursors. The reaction of two equivalents of the freshly prepared functionalized silane NSi^{Me}-H, (4-methylpyridine-2-yloxy)dimethylsilane, (**1**) [10] with half equivalent of [Rh(μ-

Cl)(coe)₂]₂ (coe = *cis*-cyclooctene) in toluene quantitatively gives the rhodium(III) species [Rh(Cl)(κ²-NSi^{Me})₂] (**2**) (NSi^{Me} = 4-methylpyridine-2-iloxy)dimethylsilyl) (Scheme 1). ¹H NMR studies of this reaction showed the presence of free coe and the formation of cyclooctane (coa) along with **2**.



Scheme 1. Synthesis of the rhodium complexes **2** and **3**.

Species **2** reacts with one equivalent of silver trifluoroacetate in CH₂Cl₂ to afford the compound [Rh(CF₃CO₂)(κ²-NSi^{Me})₂] (**3**), which has been isolated as a white solid in 73 % yield (Scheme 1). Complexes **2** and **3** have been fully characterized by elemental analysis, ¹H, ¹³C and ²⁹Si NMR spectroscopy and in the case of **3** by X-ray diffraction methods (Figure 2).

The rhodium atom in complex **3** exhibits a distorted octahedral geometry, with the oxygen atoms of the carboxylate ligand and the silicon atoms in the equatorial plane, and apical positions fulfilled by nitrogen atoms. The rhodium-silicon bond lengths in **3** are in the range 2.2277(8)-2.2388(10) Å. The (κ²-O) coordination of the carboxylate ligand to the metal is characterized by two long but similar Rh-O bond lengths (around 2.4 Å) and *trans* Si-Rh-O angles close to 160°. The pyridinic rings around the metallic centers in **3** are *trans* disposed one to each other, with similar Rh-N bond lengths (2.062(3)-2.056(3) Å). The N-Rh-N arrangement is deviated from the ideal value of

180° (N(1)-Ir(1)-N(2), 173.42(10)°), which could be related to the chelating bonding of NSi^{Me} ligands which leads to the formation of two Ir-Si-O-C-N metallacycles, with ring puckering parameters typical of ²T₁ and ²T₁ with a small contribution of ²E conformations, respectively [11].

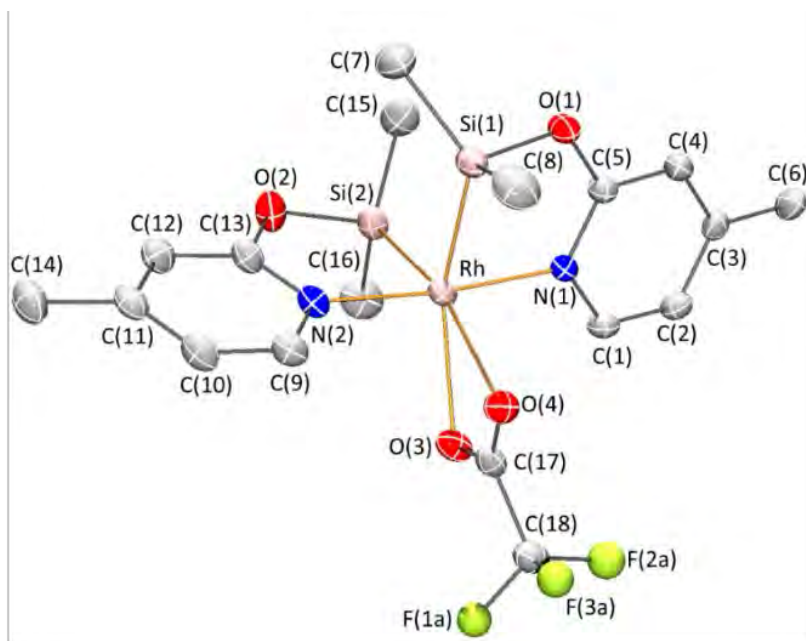
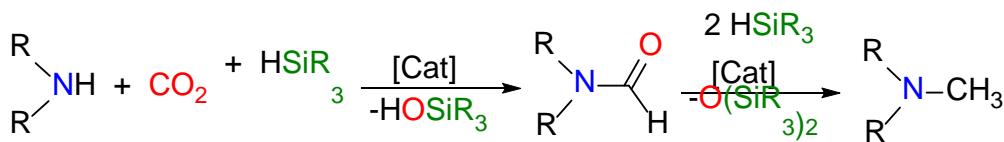


Figure 2. Molecular structure of complex **3**. Hydrogen atoms have been omitted for clarity. Selected bond lengths (Å) and angles (°): Rh-Si(1), 2.2277(8); Rh-Si(2), 2.2388(10); Rh-O(3), 2.414(2); Rh-O(4), 2.391(2); Rh-N(1), 2.062(3); Rh-N(2), 2.056(3); Si(1)-Rh-Si(2), 91.47(3); Si(1)-Rh-O(3), 158.19(6); Si(1)-Rh-O(4), 104.21(6); Si(1)-Rh-N(1), 81.82(7); Si(1)-Rh-N(2), 93.56(7); Si(2)-Rh-O(3), 109.59(6); Si(2)-Rh-O(4), 163.86(6); Si(2)-Rh-N(1), 93.51(8); Si(2)-Rh-N(2), 81.88(8); O(3)-Rh-O(4), 55.29(7); O(3)-Rh-N(1), 91.03(9); O(3)-Rh-N(2), 94.93(9); O(4)-Rh-N(1), 92.47(9); O(4)-Rh-N(2), 93.21(10); N(1)-Rh-N(2), 173.42(10).

The mononuclear structure proposed in Scheme 1 for complex **2** was corroborated by means of ^1H -DOSY NMR spectroscopy [12]. The resonances of the aromatic protons of the NSi^{Me} ligand in CD_2Cl_2 were used for the determination of the diffusion coefficients (D) of complexes **2** and **3** at 300 K. The D value measured for **2** in CD_2Cl_2 , $1.163 \times 10^{-9} \text{ m}^2 \text{ s}^{-1}$, compares well with the D value obtained for **3** under the same conditions, $1.186 \times 10^{-9} \text{ m}^2 \text{ s}^{-1}$. Therefore, assuming the mononuclear structure found for **3** (Figure 2), it is reasonable to propose that **2** also possesses a mononuclear structure in solution. In addition, ^1H and ^{13}C NMR spectra of complexes **2** and **3** also support the structure proposed for these species. $^{29}\text{Si}\{^1\text{H}\}$ NMR spectra show a doublet resonance at δ 85.7 ppm ($^1J_{\text{Rh-Si}} = 36.6 \text{ Hz}$) and δ 86.2 ppm ($^1J_{\text{Rh-Si}} = 39.3 \text{ Hz}$), respectively, which agrees with the equivalence of the two silicon atoms in both complexes.

3-Catalyzed reaction of secondary amines with hydrosilanes.

The development of catalytic methodologies that allow the utilization of CO_2 as C1 raw material for organic synthesis is of great interest [13]. The reaction of amines with CO_2 and hydrosilanes has proven to be an effective methodology for obtaining formamides, methylamines, amins and/or carbamates [14]. Thus, in presence of a catalyst, secondary and/or primary amines usually react with CO_2 and hydrosilanes to yield formamides. Furthermore, some catalysts can reduce the formamide to the corresponding methylamine (Scheme 2) [14].



Scheme 2. Catalytic formylation of secondary aliphatic amines (R_2NH) with CO_2 and hydrosilanes.

In recent years, it has been demonstrated that silylcarbamates could also be obtained from the catalytic reaction of amines with CO_2 and hydrosilanes. The formation of silylcarbamates as minor by-products of the transition metal catalyzed formylation of secondary amines with CO_2 and hydrosilanes was first observed by García et al in 2013 [15]. Few years later, we found that using the iridium complex $[\text{Ir}(\text{H})(\text{CF}_3\text{SO}_3)(\text{NSiN})(\text{coe})]$ (NSiN = *fac*-bis-(pyridine-2-yloxy)methylsilyl; *coe* = *cis*-cyclooctene) as catalyst (1.0 mol%), it was possible to selective and quantitatively prepare the corresponding silylcarbamate from the reaction of aliphatic secondary amines with CO_2 (3 bar) and one equivalent of $\text{HSiMe}(\text{OSiMe}_3)_2$ under solvent-free conditions [5]. Examples of heterogeneous catalytic systems based on 10% wt Pd on dry matrix carbon have also proven to be effective for the dehydrogenative formation of silyl carbamates from amines, CO_2 and hydrosilanes [16].

In this context, it has been found that complexes **2** and **3** (1.0 mol%) catalyze the selective reaction of pyrrolidine with CO_2 and HSiMe_2Ph to give the corresponding silylcarbamate $c\text{-(C}_4\text{H}_8\text{)NCO}_2\text{SiMe}_2\text{Ph}$ (**4a**). The ancillary ligand plays a role on the catalytic activity. Thus, complex **3** with a trifluoroacetate ligand allows the conversion of 94% of the starting silane after 6 hours, while using **2** around 80% of conversion was obtained in the same time.

The above described outcomes aimed us to explore the performance of the catalytic system based on **3**. The activity of the **3**-catalyzed reaction of pyrrolidine with CO₂ and hydrosilanes depends on the nature of the silicon compound. In all the cases, the reactions were selective to the formation of the corresponding silylcarbamate *c*-(C₄H₈)NCO₂SiR₃ (SiR₃ = SiMe₂Ph, **4a**; SiMePh₂, **5**; SiEt₃, **6**; SiMe(OSiMe₃)₂, **7**). HSiMe₂Ph is more reactive than HSiMePh₂ and HSiEt₃, and using HSiMe(OSiMe₃)₂ only 12% of the corresponding silylcarbamate **7** was observed after 24 h (Figure 3). This reactivity trend could be explained considering the lower hinderance around the Si-H bond in HSiMe₂Ph in comparison with the other silicon derivatives studied.

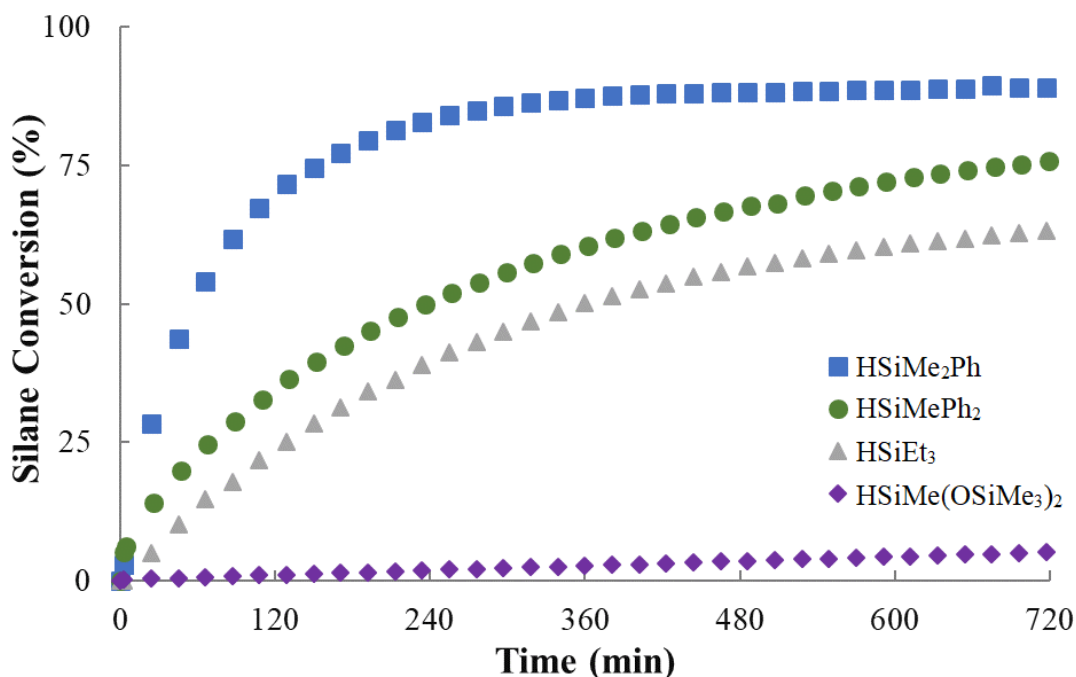
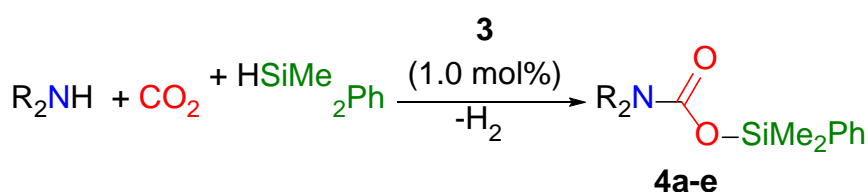


Figure 3. Representation of hydrosilane conversion (mol %) to *c*-(C₄H₈)NCO₂SiR₃ (SiR₃ = SiMe₂Ph, **4a**; SiMePh₂, **5**; SiEt₃, **6**; SiMe(OSiMe₃)₂, **7**) vs time for the **3**-catalyzed (1.0 mol%) reaction of pyrrolidine with CO₂ (3 bar) and the corresponding silane at 323K in C₆D₆.

^1H NMR studies of the reaction of pyrrolidine with CO_2 (3 bar) and HSiMe_2Ph in C_6D_6 at 323 K in presence of 0.5, 1.0 and 5.0 mol% of **3** evidenced that the catalyst loading moderately influences on the catalytic activity (Figure S39). In addition, it has been found that the nature of the amine strongly influences the catalytic activity, where the best results were obtained for cyclic secondary amines such as pyrrolidine and piperidine, while the reactions with *N,N*-diisopropylamine bearing a hindered N-H bond were slower (Table 1 and Figure 4). In addition, no reaction was observed with *N*-methylaniline.



Scheme 3. Preparation of silylcarbamates from the **3**-catalyzed (1.0 mol%) reaction of secondary amines with CO_2 (3 bar) and HSiMe_2Ph in C_6D_6 at 323 K. ($\text{R}_2 = c\text{-(C}_4\text{H}_8)$, **4a**; $c\text{-(C}_4\text{H}_8\text{O)}$, **4b**; $c\text{-(C}_5\text{H}_{10})$, **4c**; Et_2 , **4d**; $i\text{Pr}_2$, **4e**).

The silylcarbamates **4a-e**, **5** and **6** were characterized by means of ^1H , ^{13}C and ^{29}Si NMR spectroscopy (see experimental and supporting). Compound **7** was characterized by comparison with the reported data [5]. The most noticeable resonances in their $^{13}\text{C}\{^1\text{H}\}$ NMR spectra were those corresponding to the carboxylic carbon atom that appears around δ 154 ppm, which agrees with the reported data for analogous compounds [5].

Table 1: Selectivity to silylcarbamate from the **3**-catalyzed (1.0 mol%) reaction of secondary amines with CO₂ (3 bar) and HSiMe₂Ph in C₆D₆ at 323 K.

Amine	Carbamate; (%) ^[a]	Conversion, % ^[b]	Formamide, % ^[a]
Pyrrolidine	4a ; (99)	94	1
Morpholine	4b ; (96)	78	3
Piperidine	4c ; (97)	80	4
<i>N,N</i> -diethylamine	4d ; (97)	92	3
<i>N,N</i> -diisopropylamine	4e ; (100)	36	-

[a] mol% base on ¹H NMR integration; [b] mol% of the starting amine consumed after 14 hours of reaction.

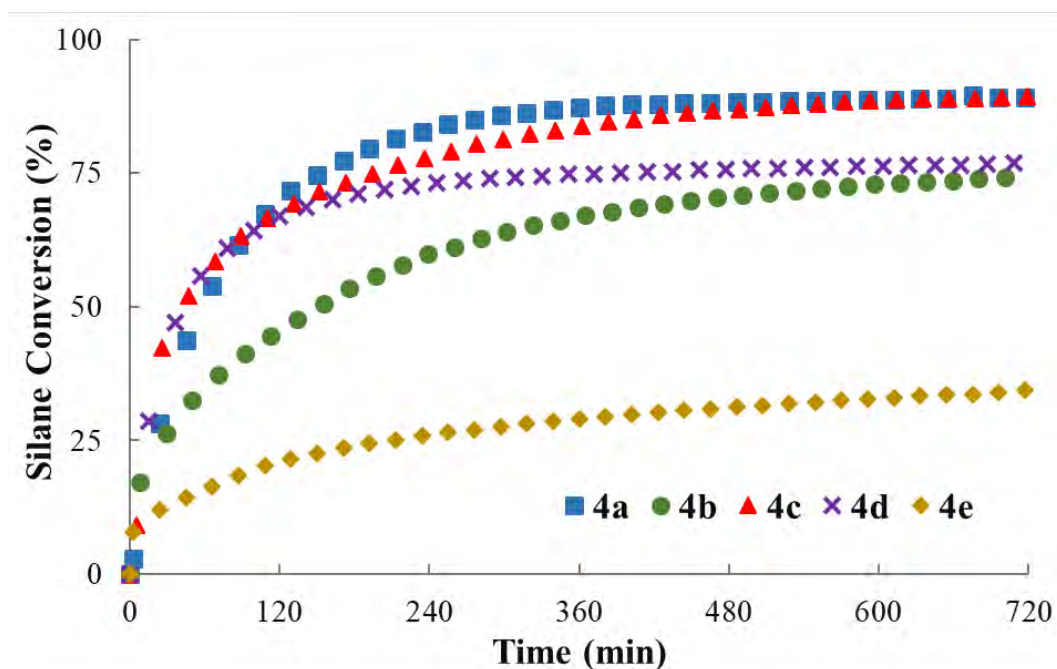
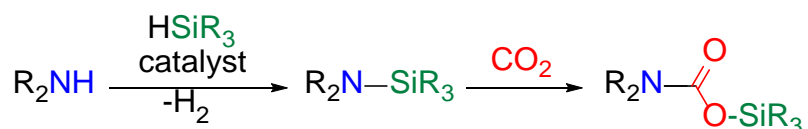


Figure 4. Representation of HSiMe₂Ph conversion (mol %) to R₂NCO₂SiMe₂Ph (R₂ = *c*-(C₄H₈), **4a**; *c*-(C₄H₈O), **4b**; *c*-(C₅H₁₀), **4c**; Et₂, **4d**; ⁱPr₂, **4e**) vs time for the **3**-catalyzed (1.0 mol%) reaction of secondary amines with CO₂ (3 bar) and HSiMe₂Ph at 323K in C₆D₆.

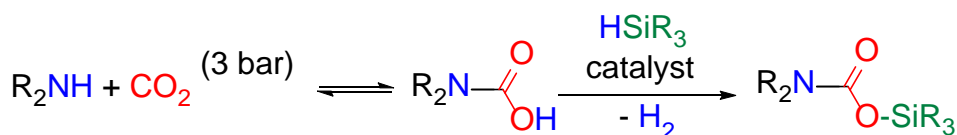
In the absence of complexes **2** and **3**, C₆D₆ solutions of pyrrolidine and HSiMe₂Ph react with CO₂ (3 bar) to quantitatively give a mixture of the corresponding carbamic acid and HSiMe₂Ph. This mixture slowly evolves at 323 K to produce the corresponding silylcarbamate and traces of formamide. Thus, after 60 hours a 36% of conversion of the carbamic acid into silylcarbamate (30%) and a formamide (6%) is observed. These outcomes prove that species **2** and **3** play a relevant role on the above-mentioned catalytic process.

Two different reaction pathways have been proposed to explain the catalytic formation of silylcarbamates from the reaction of amines with CO₂ and hydrosilanes (Scheme 4). The first one consists in the insertion of a CO₂ molecule into the Si-N bond of an *in situ* generated silylamine (Scheme 4, *path a*) [5, 17, 18, 19]. This path requires a previous step consisting in a dehydrogenative silylation of the amine [20, 21]. The second possibility is the catalytic dehydrogenative silylation of the corresponding carbamic acid (Scheme 4, *path b*).

a) Silylamine route to silylcarbamate



b) Carbamic acid route to silylcarbamate



Scheme 4. Possible reaction paths for the catalytic formation of silylcarbamates from aliphatic secondary amines (R₂NH), CO₂ and hydrosilanes.

It has been demonstrated that, differently to that observed for Ir-N₂Si based catalysts [5], in absence of CO₂, solutions of pyrrolidine and HSiMe₂Ph in presence of catalytic

amounts of **3** (1.0 mol%) are stable over time. Indeed, no reaction was observed after 6 h at 343 K. Analogous behavior was observed for piperidine and morpholine. Therefore, under the studied conditions complex **3** is not an active catalyst for the dehydrogenative silylation of secondary amines. Therefore, it is reasonable to discard *path a* of Scheme 4 for explaining the formation of silylcarbamates.

It is worth mentioning that under the reaction conditions, 3 bar of CO₂, the equilibrium between the amine and the corresponding carbamic acid [22] is shifted towards the latter (Figure 5). This suggest that formation of the silylcarbamate could be consequence of the **3**-catalyzed dehydrogenative silylation of the corresponding carbamic acid according to *path b* in Scheme 4.

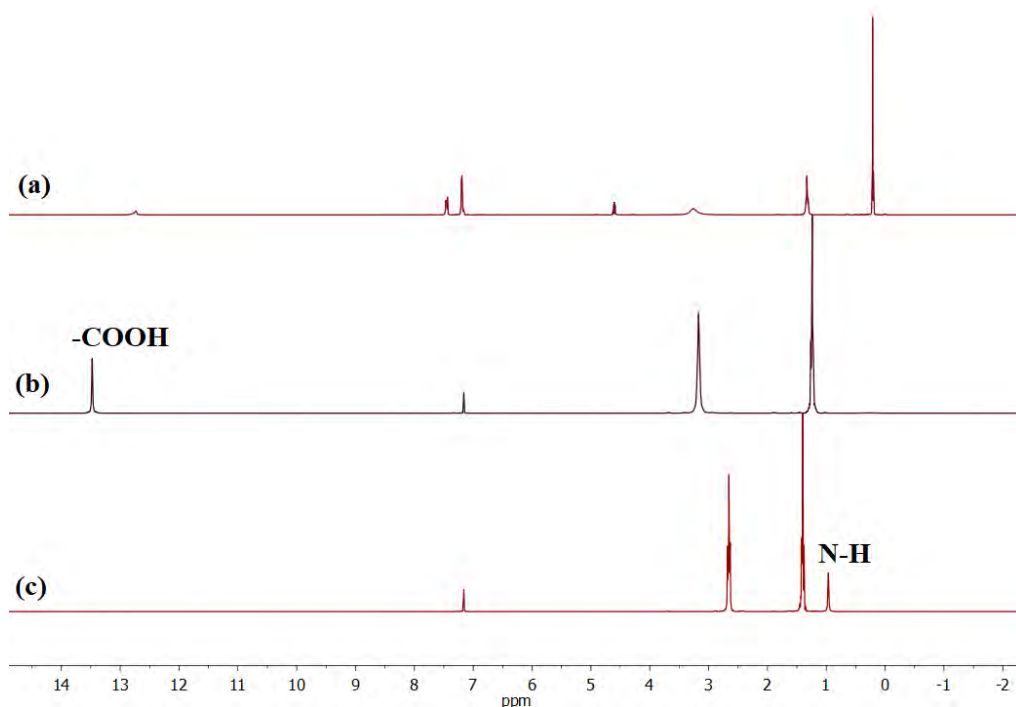
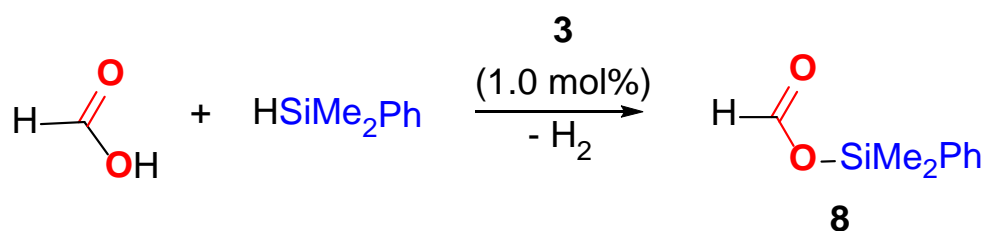


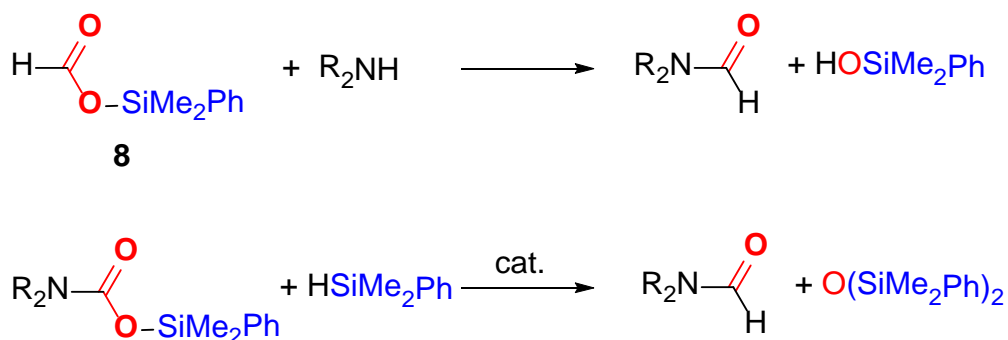
Figure 5. (a) ¹H NMR spectrum of the **3** catalyzed reaction of pyrrolidine, CO₂ (3 bar) and HSiMe₂Ph before heating. (b) ¹H NMR spectrum of pyrrolidine under atmosphere of CO₂ (3 bar) in C₆D₆ at 298 K. (c) ¹H NMR spectrum of pyrrolidine in C₆D₆ at 298K.

In agreement with that possibility, it has been proven that, similarly to other group 9 metal complexes [6], species **3** catalyzes the dehydrogenative silylation of formic acid to afford the silylformate HCO₂SiMe₂Ph (**8**). Thus, the **3**-catalyzed (1.0 mol%) reaction of formic acid with one equivalent of HSiMe₂Ph quantitatively affords **8** and H₂ (Scheme 5). The silylformate **8** has been characterized by comparison of its ¹H NMR spectra with reported data [3a].



Scheme 5. Dehydrogenative silylation of formic acid with HSiMe₂Ph catalyzed by **3** (1.0 mol%).

Table 1 illustrates that formamides were obtained as minor side products of these reactions in around 1-4% yield. The obtention of formamides from the catalytic reaction of secondary amines with CO₂ using hydrosilanes as reductants, has been commonly explained because of the reaction of the *in situ* produced silylformates, by CO₂ hydrosilylation, with the corresponding amine [13], or by the catalytic reaction of silylcarbamates with hydrosilanes to yield formamides and the corresponding siloxane [23] (Scheme 6).



Scheme 6. Possible pathways to explain the formation of formamides as side reaction products.

In this regard, it should be mentioned that the ^1H NMR studies of the **3**-catalyzed reaction of CO_2 (3 bar) with HSiMe_2Ph in C_6D_6 at 323 K revealed that after 24 hours of reaction only traces of the corresponding silylformate **8** were formed. Moreover, the **3**-catalyzed reaction of pyrrolidine with CO_2 (3 bar) in presence of four equivalents of HSiMe_2Ph quantitatively affords the silylcarbamate **4a**, which did not react with the excess of HSiMe_2Ph present in the reaction mixture, even after 24 hours at 323 K. Therefore, the low concentration of formamide observed along the above described reactions (Table 1) could be consequence of the poor activity of **3** as CO_2 and/or silylcarbamates hydrosilylation catalyst.

3 Experimental

General information. All manipulations were performed with rigorous exclusion of air at an argon/vacuum manifold using standard Schlenk-tube techniques or in MBraun glovebox when necessary. Solvents were dried and distilled under argon by standard procedures prior to use or purified by a Solvent Purification System (Innovative Technologies). NMR spectra were obtained on a Bruker ARX-300, Bruker AV-300 MHz or Varian Gemini 2000. Chemical shifts (δ), reported in ppm, were referenced to the residual peaks of deuterated solvents. Compound **1** was prepared according to the

method reported in the literature [10]. HSiMe₂Ph and carbon dioxide (99.99 % purity) were purchased from commercial sources.

Synthesis of [Rh(Cl)(κ²-NSi^{Me})₂] (2). A toluene solution (5 mL) of compound **1** (0.300 g, 1.800 mmol) was slowly added to a suspension of [Rh(μ-Cl)(coe)₂]₂ (0.760 g, 0.848 mmol) in toluene (10 mL) and the resulting mixture was stirred at room temperature for 2 h. The solvent was removed *in vacuo* and the residue washed with pentane cooled at 273 K (3 x 10 mL) to afford a pale brown solid. Yield: 0.320 g (76%). Anal. Calcd. for C₁₆H₂₄ClRhN₂O₂Si₂: C, 40.81; H, 5.14; N, 5.95. Found: C, 40.84; H, 5.15; N, 6.09. ¹H NMR plus HSQC ¹H-¹³C (300 MHz, 298 K, CD₂Cl₂): δ 8.58 (d, ³J_{H-H} = 6.1 Hz, 2H, py-6), 6.67 (m, 2H, py-3), 6.59 (dd, ³J_{H-H} = 6.1 Hz, ⁵J_{H-H} = 1.8 Hz, 2H, py-5), 2.30 (s, 6H, CH₃-py), 0.65 (s, 6H, SiMe), 0.40 (s, 6H, SiMe). ¹³C{¹H} APT plus HSQC ¹H-¹³C (75 MHz, 298 K, CD₂Cl₂): δ 166.8 (s, C₂-py), 152.8 (s, C₄-py), 150.3 (s, C₆-py), 118.4 (s, C₅-py), 112.0 (s, C₃-py), 21.3 (s, CH₃-py), 6.8 (s, SiMe), 3.8 (d, ²J_{Rh-H} = 4.0 Hz, SiMe). ²⁹Si{¹H} NMR (HMBC ¹H-²⁹Si, 298 K, CD₂Cl₂): δ 85.7 (d, ¹J_{Rh-Si} = 36.6 Hz). High Resolution Mass Spectrometry (ESI⁺): calc. *m/z* = 435.0432; found *m/z* = 434.9765 (M⁺-Cl).

Synthesis of [Rh(CF₃CO₂)(κ²-NSi^{Me})₂] (3). CH₂Cl₂ (15mL) was added to a light-protected Schlenk tube containing a mixture of complex **2** (0.300 g, 0.320 mmol) and silver trifluoroacetate (0.150 g, 0.680 mmol). The resulting suspension was stirred at room temperature for 4 h and filtered out through celite. The solvent was removed *in vacuo* and the residue washed with cold pentane (198 K, 3 x 10 mL) to afford a white solid. Yield 0.255 g (73 %). Anal. Calcd. for C₁₈H₂₄F₃RhN₂O₄Si₂: C, 39.42; H, 4.41; N, 5.11. Found: C, 39.32; H, 4.25; N, 4.98. ¹H NMR plus HSQC ¹H-¹³C (300 MHz, 298 K, CD₂Cl₂): δ 7.96 (d, ³J_{H-H} = 6.0 Hz, 2H, py-6), 6.69 (s, 2H, py-3), 6.67 (d, ³J_{H-H} = 6.0 Hz, 2H, py-5), 2.30 (s, 6H, CH₃-py), 0.61 (s, 6H, SiMe), 0.41 (s, 6H, SiMe).

$^{13}\text{C}\{^1\text{H}\}$ NMR APT plus HSQC ^1H - ^{13}C (75 MHz, 298 K, CD_2Cl_2): δ 166.7 (s, C_2 -py), 153.1 (s, C_4 -py), 147.7 (s, C_6 -py), 118.9 (s, C_5 -py), 112.4 (s, C_3 -py), 21.3 (s, CH_3 -py), 4.6 (s, SiMe), 3.2 (d, $^2J_{\text{Rh-H}} = 4.4$ Hz, SiMe). $^{19}\text{F}\{^1\text{H}\}$ NMR (282 MHz, 298 K, CD_2Cl_2): δ -75.6 (CF_3CO_2). ^{29}Si NMR (HMBC ^1H - ^{29}Si , 298 K, CD_2Cl_2): δ 86.2 (d, $^1J_{\text{Rh-Si}} = 39.3$ Hz). High Resolution Mass Spectrometry (ESI⁺): calc. $m/z = 435.0432$; found $m/z = 435.0423$ ($\text{M}^+ - \text{CF}_3\text{CO}_2$).

3-catalyzed (1.0 mol%) reactions. A Young cap NMR tube was filled with the catalyst precursor **3** (2.00 mg, 3.64 μmol), HSiMe_2Ph (0.401 mmol, 61.5 μL), amine (0.364 mmol) and 0.5 mL of C_6D_6 . Argon was removed under reduced pressure after freezing the solution, and the tube was then pressurized with CO_2 (3 bar) and heated to 323 K. The same procedure was followed for the reactions of pyrrolidine with other silanes (HSiMePh_2 , 80.0 μL ; HSiEt_3 , 64 μL ; $\text{HSiMe}(\text{OSiMe}_3)_2$, 109.0 μL).

3-catalyzed (1.0 mol%) dehydrogenative silylation of formic acid. A Young cap NMR tube was filled with the catalyst precursor **3** (2.00 mg, 3.64 μmol), HSiMe_2Ph (0.401 mmol, 61.5 μL), formic acid (0.364 mmol, 13.7 μL) and 0.5 mL of C_6D_6 . The mixture was then heated at 323 K and monitored by ^1H NMR spectroscopy.

Selected NMR data of the catalytic products.

***c*-(C_4H_8) $\text{N-C(O)OSiMe}_2\text{Ph}$ (**4a**).** ^1H NMR (300 MHz, C_6D_6 , 298 K): δ 7.78 – 7.75 (m, 2H, Ph), 7.28 – 7.20 (m, 3H, Ph), 3.23 – 3.05 (m, 4H, N- CH_2), 1.24 – 1.20 (m, 4H, - CH_2 -), 0.66 (s, 6H, SiCH_3). ^{13}C NMR APT (75 MHz, C_6D_6): δ 153.6 (s, CO_2Si), 137.4 (s, $C_{\text{ipso}}\text{-Ph}$), 134.1 (s, Ph), 130.1 (s, Ph), 128.2 (s, Ph), 46.5 (s, N- CH_2), 46.1 (s, N- CH_2), 25.7 (s, CH_2), 25.1 (s, CH_2), -0.8 (s, SiCH_3). $^{29}\text{Si}\{^1\text{H}\}$ NMR (HMBC ^{29}Si - ^1H , 298 K): δ 9.8 (s, SiCH_3).

c-(C₄H₈O)N-C(O)OSiMe₂Ph (4b). ¹H NMR (300 MHz, C₆D₆, 298 K): δ 7.71 – 7.68 (m, 2H, Ph), 7.25 – 7.21 (m, 3H, Ph), 3.23 – 3.13 (m, 8H, -CH₂-), 0.61 (s, 6H, SiCH₃). ¹³C NMR APT (75 MHz, C₆D₆): δ 154.0 (s, CO₂Si), 136.8 (s, C_{ipso}-Ph), 134.1 (s, Ph), 130.3 (s, Ph), 128.2 (s, Ph), 66.4 (s, O-CH₂), 45.3 (s, N-CH₂), 44.0 (s, N-CH₂), -1.1 (s, SiCH₃). ²⁹Si{¹H} NMR (HMBC ²⁹Si-¹H, 298 K): δ 10.9 (s, SiCH₃).

c-(C₅H₁₀)N-C(O)OSiMe₂Ph (4c). ¹H NMR (300 MHz, C₆D₆, 298 K): δ 7.74 – 7.71 (m, 2H, Ph), 7.24 – 7.21 (m, 3H, Ph), 3.28 (br s, 4H, N-CH₂), 1.13 (br s, 6H, -CH₂-), 0.63 (s, 6H, SiCH₃). ¹³C NMR APT (75 MHz, C₆D₆): δ 154.1 (s, CO₂Si), 137.3 (s, C_{ipso}-Ph), 134.1 (s, Ph), 130.3 (s, Ph), 128.2 (s, Ph), 45.8, 44.7 (s, N-CH₂), 26.1, 25.7 (s, -CH₂-), 24.4 (s, -CH₂-), -0.9 (s, SiCH₃). ²⁹Si{¹H} NMR (HMBC ²⁹Si-¹H, 298 K): δ 10.0 (s, SiCH₃).

Et₂N-C(O)OSiMe₂Ph (4d). ¹H NMR (300 MHz, C₆D₆, 298 K): δ 7.72 – 7.69 (m, 2H, Ph), 7.25 – 7.19 (m, 3H, Ph), 3.11 – 2.98 (m, 4H, N-CH₂), 0.89 (br, 6H, CH₃), 0.61 (s, SiCH₃). ¹³C NMR APT (75 MHz, C₆D₆): δ 154.6 (s, CO₂Si), 137.4 (s, C_{ipso}-Ph), 134.0 (s, Ph), 130.1 (s, Ph), 128.2 (s, Ph), 42.0, 41.7 (s, N-CH₂), 14.3, 13.5 (s, CH₃), -0.9 (s, SiCH₃). ²⁹Si{¹H} NMR (HMBC ²⁹Si-¹H, 298 K): δ 10.1 (s, SiCH₃).

ⁱPr₂N-C(O)OSiMe₂Ph (4e). ¹H NMR (300 MHz, C₆D₆, 298 K): δ 7.74 – 7.71 (m, 2H, Ph), 7.23 – 7.19 (m, 3H, Ph), 3.90 – 3.56 (m, 2H, N-CH), 1.04 (d, *J* = 6.8 Hz, 12H, CH₃), 0.62 (s, SiCH₃). ¹³C NMR APT (75 MHz, C₆D₆): δ 154.2 (s, CO₂Si), 137.5 (s, C_{ipso}-Ph), 134.1 (s, Ph), 130.0 (s, Ph), 128.1 (s, Ph), 46.2 (s, N-CH), 21.5, 20.5 (br s, CH₃), -0.8 (s, SiCH₃). ²⁹Si{¹H} NMR (HMBC ²⁹Si-¹H, 298 K): δ 9.4 (s, SiCH₃).

c-(C₄H₈)N-C(O)OSiMePh₂ (5). ¹H NMR (300 MHz, C₆D₆, 298 K): δ 7.84 – 7.82 (m, 4H, Ph), 7.25 – 7.24 (m, 6H, Ph), 3.29 (br s, 4H, N-CH₂), 1.36 (m, 4H, CH₂), 0.99 (s, 3H, SiCH₃). ¹³C NMR APT (75 MHz, C₆D₆): δ 153.2 (s, CO₂Si), 137.9 (s, C_{ipso}-Ph),

135.1 (s, Ph), 130.3 (s, Ph), 128.2 (s, Ph), 46.2 (br s, N-CH₂), 25.4 (br s, CH₂), 25.2 (s, CH₂), -1.7 (s, SiCH₃). ²⁹Si{¹H} NMR (HMBC ²⁹Si-¹H, 298 K): δ -1.0 (s, SiCH₃).

c-(C₄H₈)N-C(O)OSiEt₃ (6). ¹H NMR (300 MHz, C₆D₆, 298 K): δ 3.23 – 3.10 (m, 4H, N-CH₂), 1.06 (m, 9H, CH₃), 0.86 (s, 6H, SiCH₂). ¹³C NMR APT (75 MHz, C₆D₆): δ 153.7 (s, CO₂Si), 46.5 (s, N-CH₂), 46.1 (s, N-CH₂), 25.8 (s, CH₂), 25.2 (s, CH₂), 8.4 (s, CH₃), 5.4 (s, SiCH₂). ²⁹Si{¹H} NMR (HMBC ²⁹Si-¹H, 298 K): δ 22.3 (s, SiCH₃).

Crystal Structure Determination of Complex 3.

X-ray diffraction data were collected at 100(2)K on an automatic Smart APEX Bruker diffractometer with graphite-monochromated Mo K α radiation ($\lambda=0.71073$ Å) using ω scans with narrow oscillation frames (0.3°). Diffracted intensities were integrated and corrected from absorption effects with SAINT+ [24] and SADABS [25] programs, included in APEX 3 package. The structure was solved by direct methods and refined with SHELXS-2013 [26] and refined with full-matrix least-squares refinement with SHELXL-2018 [27] programs included in WingX package [28].

Crystal Data for **3**: C₁₈H₂₄F₃N₂O₄RhSi₂; Mr = 548.48; yellow prism, 0.180 × 0.200 × 0.215 mm; Orthorhombic *Pna21*; a = 20.5601(9) Å, b = 8.1427(4) Å, c = 14.0964(6) Å; V = 2359.94(18) Å³; Z = 4; $\rho_{\text{calcd}} = 1.544$ g cm⁻³; $\mu = 0.874$ cm⁻¹; minimum and maximum transmission factors 0.8164 and 0.8749; $2\theta_{\text{max}} = 58.028^\circ$; 43100 reflections collected; 5994 unique reflections ($R_{\text{int}} = 0.0212$); number of data/restraints/parameters 5994/1/289; final *GOF* = 1.050; $R_I = 0.0226$ [5848 reflections, $I > 2\sigma(I)$], $wR2 = 0.0536$ for all data; largest difference peak 0.657 e Å⁻³.

Hydrogen atoms were included in the model in calculated positions and refined with a riding model. Fluorine atoms have been found to be disordered. They have been

included in the model in three sets of positions with 0.42/0.30/0.28(1) occupancy factors and isotropically refined.

CCDC 1906237 contains the supplementary crystallographic data for this paper. The data can be obtained free of charge from The Cambridge Crystallographic Data Centre via www.ccdc.cam.ac.uk/structures.

4 Conclusions

The reaction of (4-methyl-pyridine-2-iloxy)dimethylsilane ($\text{NSi}^{\text{Me}}\text{-H}$, **1**) with $[\text{RhCl}(\text{coe})_2]_2$ gives $[\text{Rh}(\text{Cl})(\kappa^2\text{-NSi}^{\text{Me}})_2]$ (**2**), which reacts with a stoichiometric amount of AgCF_3CO_2 to afford $[\text{Rh}(\kappa^2\text{-CF}_3\text{CO}_2)(\kappa^2\text{-NSi}^{\text{Me}})_2]$ (**3**). Complexes **2** and **3** have been fully characterized by elemental analysis and NMR spectroscopy. In addition, the solid-state structure of **3** has been confirmed by X-ray diffraction studies.

Complex **3** is an effective catalyst for the selective formation of silylcarbamates from the reaction of aliphatic secondary amines with CO_2 and hydrosiloxanes. Moreover, it has been demonstrated that **3** is an active catalyst for dehydrogenative silylation of carboxylic acids. However, under the studied conditions, **3** is a poor catalyst for the hydrosilylation of CO_2 and for the dehydrogenative silylation of amines.

These outcomes allow to conclude that the **3**-catalyzed dehydrogenative silylation of the carbamic acid *in situ* generated by reaction of the corresponding secondary amine with CO_2 is the determining step for explaining the selective formation of silylcarbamates from the **3**-catalyzed reaction of secondary amines with CO_2 and HSiMe_2Ph .

Acknowledgements

The financial support from MINECO/FEDER project CTQ2015-67366-P and DGA/FSE project E42_17R is gratefully acknowledged. Dr. P. García-Orduña acknowledges CSIC, European Social Fund and Ministerio de Economía y Competitividad of Spain for a PTA contract. Authors would like to acknowledge the use of Servicio General de Apoyo a la Investigación-SAI, Universidad de Zaragoza.

References

- [1] L. Ehrlich, R. Gericke, E. Brendler, J. Wagler, *Inorganics* 6 (2018) 119, doi: 10.3390/inorganics6040119.
- [2] F. J. Fernández-Alvarez, R. Lalrempuia, Luis A. Oro, *Coord. Chem. Rev.* 350 (2017) 49 – 60.
- [3] (a) A. Julián, J. Guzmán, E. A. Jaseer, F. J. Fernández-Alvarez, R. Royo, V. Polo, P. García-Orduña, F. J. Lahoz, L. A. Oro, *Chem. Eur. J.* 23 (2017) 11898 – 11907; (b) A. Julián, E. A. Jaseer, K. Garcés, F. J. Fernández-Alvarez, P. García-Orduña, F. J. Lahoz, L. A. Oro, *Catal. Sci. Technol.* 6 (2016) 4410 – 4417; (c) R. Lalrempuia, M. Iglesias, V. Polo, P. J. Sanz Miguel, F. J. Fernández-Alvarez, J. J. Pérez-Torrente, L. A. Oro, *Angew. Chem. Int. Ed.* 51 (2012) 12824 – 12827.
- [4] K. Garcés, F. J. Fernández-Alvarez, V. Polo, R. Lalrempuia, J. J. Pérez-Torrente, L. A. Oro, *ChemCatChem* 6 (2014) 1691 – 697.

- [5] A. Julián, V. Polo, E. A. Jaseer, F. J. Fernández-Alvarez, L. A. Oro, *ChemCatChem* 7 (2015) 3895 – 3902.
- [6] A. Julián, K. Garcés, R. Lalrempuia, E. A. Jaseer, P. García-Orduña, F. J. Fernández-Alvarez, F. J. Lahoz, L. A. Oro, *ChemCatChem* 10 (2018) 1027 – 1034.
- [7] A. Julián, V. Polo, F. J. Fernández-Alvarez, L. A. Oro, *Catal. Sci. Technol.* 7 (2017) 1372 – 1378.
- [8] K. Garcés, R. Lalrempuia, V. Polo, F. J. Fernández-Alvarez, P. García-Orduña, F. J. Lahoz, J. J. Pérez-Torrente, L. A. Oro, *Chem. Eur. J.* 22 (2016) 14717 – 14729.
- [9] J. Guzmán, A. M. Bernal, P. García-Orduña, F. J. Lahoz, L. A. Oro, F. J. Fernández-Alvarez, *Dalton Trans.* 48 (2019) 4255 – 4262.
- [10] J. Guzmán, P. García-Orduña, V. Polo, F. J. Lahoz, L. A. Oro, F. J. Fernández-Alvarez, *Catal. Sci. Technol.* 9 (2019) 2858 – 2867.
- [11] D. Cremer, J. A. Pople, *J. Am. Chem. Soc.* 97 (1975) 1354 – 1358.
- [12] G. A. Morris, Diffusion-Ordered Spectroscopy. In *Encyclopedia of Magnetic Resonance*; R. K. Harris; R. E. Wasylshen, Eds.; Wiley: Chichester, U.K., 2009.
- [13] (a) N. A. Tappe, R. M. Reich, V. D'Elia, F. E. Kühn, *Dalton Trans.*, 47 (2018) 13281-13313; (b) T. P. Senftle, E. A. Carter, *Acc. Chem. Res.* 50 (2017) 472–475; (c) Carbon Dioxide and Organometallics, (Ed.: X.-B. Lu), *Top. Organomet. Chem.*, vol. 53, Springer International Publishing Switzerland, Heidelberg, 2016; (d) M. Cokoja, C. Bruckmeier, B. Rieger, W. A. Herrmann, F. E. Kühn, *Angew. Chem. Int. Ed.* 50 (2011) 8510 – 8537; (e) Carbon Dioxide as Chemical Feedstock, (Ed., M. Aresta),

Wiley-VCH, Weinheim, 2010; (d) Q. Yi, W. Li, J. Feng, K. Xie, *Chem. Soc. Rev.* 44 (2015) 5409–5445.

[14] For recent reviews see: (a) F. J. Fernández-Alvarez, L. A. Oro, *ChemCatChem* 10, (2018) 4783 – 4796; (b) R. A. Pramudita, K. Motokura, *Green Chem.* 20 (2018) 4834 – 4843; (c) X. Frogneux, E. Blondiaux, P. Thuery, T. Cantat, *ACS Catal.* 5 (2015) 3983 – 3987; (d) A. Tlili, E. Blondiaux, X. Frogneux, T. Cantat, *Green Chem.* 17 (2015) 157 – 168; (e) I. Sorribes, K. Junge, M. Beller, *Chem. Eur. J.* 20 (2014) 7878 – 7883; (f) Y. Li, X. Fang, K. Junge, M. Beller, *Angew. Chem. Int. Ed.* 52 (2013) 9568 – 9571.

[15] L. Gonzalez-Sebastián, M. Flores-Alamo, J. J. García, *Organometallics* 32 (2013) 7186 – 7190.

[16] S. Tanaka, T. Yamamura, S. Nakane, M. Kitamura, *Chem. Commun.* 51 (2015) 13110 – 13112.

[17] (a) M. Herbig, U. Böhme, E. Kroke, *Inorg. Chim. Acta* 473 (2018) 20 – 28; (b) K. Kraushaar, C. Wiltzsch, J. Wagler, U. Böhme, A. Schwerzer, G. Roewer, E. Kroke, *Organometallics* 31 (2012) 4779 – 4785; (c) C. Wiltzsch, K. Kraushaar, A. Schwerzer, E. Kroke, *Z. Naturforsch.* 66b (2011) 917 – 922; (d) M. J. Fuchter, C. J. Smith, M. W. S. Tsang, A. Boyer, S. Saubern, J. H. Ryan, A. B. Holmes, *Chem. Commun.* (2008) 2152 – 2154.

[18] For a recent review see: K. Kraushaar, D. Schmidt, A. Schwerzer, E. Kroke, *Adv. Inorg. Chem.* 66 (2014) 117 – 162.

[19] M. Xu, A. R. Jupp, M. S. E. Ong, K. I. Burton, S. S. Chitnis, D. W. Stephan, *Angew. Chem. Int. Ed.* 58 (2019) 5707 – 5711.

[20] For a recent review on catalytic formation of silicon–heteroatom bonds see: K. Kuciński, G. Hreczycho, *ChemCatChem* 9 (2017) 1868 – 1885.

[21] (a) M. P. Cibuzar, R. Waterman, *Organometallics* 37 (2018) 4395 – 4401; (b) P. Rios, M. Roselló-Merino, O. Rivada-Wheelaghan, J. Borge, J. López-Serrano, S. Conejero, *Chem. Commun.* 54 (2018) 619 – 622; (c) L. K. Allen, R. García-Rodríguez, D. S. Wright, *Dalton Trans* 44 (2015) 12112 – 12118; (d) J. Hermele, H. F. T. Klare, M. Oestreich, *Chem. Eur. J.* 20 (2014) 9250 – 9254; (e) C. David F. Königs, M. F. Müller, N. Aiguabella, H. F. T. Klare, M. Oestreich, *Chem. Commun.* 49 (2013) 1506–1508; (f) W. Xie, H. Hu, C. Cui, *Angew. Chem. Int. Ed.* 51 (2012) 11141–11144; (g) J. F. Dunne, S. R. Neal, J. Engelkemier, A. Ellern, A. D. Sadow, *J. Am. Chem. Soc.* 133 (2011) 16782 – 16785; (h) D. V. Gutsulyak, S. F. Vyboishchikov, G. I. Nikonov, *J. Am. Chem. Soc.* 132 (2010) 5950 – 5951; (i) F. Buch, S. Harder, *Organometallics* 26 (2007) 5132 – 5135; (j) K. Takaki, K. Komeyama, K. Takehira, *Tetrahedron* 59 (2003) 10381 – 10395; (k) J. X. Wang, A. K. Dash, J. C. Berthet, M. Ephritikhine, M. S. Eisen, *J. Organomet. Chem.* 610 (2000) 49 – 57; (l) J. A. Reichl, D. H. Berry, *Advances in Organometallics Chemistry* 43 (1999) 197 – 265; (m) J. He, H. Q. Liu, J. F. Harrod, R. Hynes, *Organometallics* 13 (1994) 336 – 343; (n) H. Liu, Q. J. F. Harrod, *Organometallics* 11 (1992) 822 – 827; (o) H. Q. Liu, J. F. Harrod, *Can. J. Chem.* 70 (1992) 107 – 110; (p) L. H. Sommer, J. D. Citron, *J. Org. Chem.* 32 (1967) 2470 – 2472.

[22] M. Aresta, D. Ballivet-Tkatchenko, D. Belli Dell’Amico, M. C. Bonnet, D. Boschi, F. Calderazzo, R. Faure, L. Labella, F. Marchetti, *Chem. Commun.* (2000) 1099 – 1100.

[23] H. Lv, Q. Xing, C. Yue, Z. Lie, F. Li, *Chem. Commun.* 52 (2016) 6545 – 6548.

[24] SAINT+ in APEX3 v 2017.3, Area detector Integration Software; Bruker AXS, Madison, WI, 2008.

[25] L. Krause, R. Herbst-Irmer, G. M. Sheldrick, D. Stalke, *J. Appl. Cryst.*, 48 (2015) 3 – 10.

[26] G. M. Sheldrick, *Acta Cryst A* 64 (2008) 112 – 122.

[27] G. M. Sheldrick, *Acta Cryst*, C71 (2015) 3 – 8.

[28] L. J. Farrugia, *J. Appl. Cryst.* 45 (2012) 849 – 854.